1 **ULTRA HIGH PERFORMANCE FIBER REINFORCED CONCRETE**

2 **UNDER CYCLIC LOADING**

3

4 **Spyridon A. Paschalis and Andreas P. Lampropoulos**

5

6 **Biography:**

7 **Spyridon A. Paschalis** is a PhD candidate at the University of Brighton. He has graduated

8 from the Department of Civil Engineering of the Democritus University of Thrace (2007). He

9 holds an MSc in "Earthquake Engineering and Seismic Resistant Structures" from the

10 Hellenic Open University (2013) and he has worked as a structural engineer in the private

11 sector. His main research interest is focused on the Earthquake Strengthening of Structures.

12 **Dr Andreas P. Lampropoulos** is Senior Lecturer at the University of Brighton. He received

13 his PhD from the University of Patras in 2010. His research agenda spans the areas of

14 earthquake strengthening/retrofitting existing structures, new cement free concrete materials

15 and Ultra High Performance Fiber Reinforced Concrete (UHPFRC). He has published more

16 than 25 journal and conference papers and he serves as the Chair of IABSE Working Group 7

17 on 'Earthquake Resistant Structures'.

18

19 **ABSTRACT**

20 Ultra High Performance Fiber Reinforced Concrete (UHPFRC) is a novel cementitious

21 material with enhanced strength in tension and compression and significantly high energy

22 absorption in the post-cracking region. The application of UHPFRC for the earthquake

23 strengthening of existing structures could considerably improve the performance of existing

24 structures due to its superior properties. There are published studies where the direct tensile

25 and the flexural behavior of UHPFRC have been investigated and the superior tensile

strength and post-crack energy absorption have been highlighted. However, there are not any published studies on the performance of UHPFRC under cyclic loading. In this paper, the results of an extensive experimental program on UHPFRC under direct tensile cyclic loading are presented and a constitutive model for the response of UHPFRC under cyclic loading is proposed. The accuracy of the proposed model is validated using experimental results from various loading histories and for different percentages of fibers, and the reliability of the proposed model is highlighted.

Keywords: UHPFRC; Cyclic Loading; Direct Tensile Tests; Constitutive model

INTRODUCTION

Ultra High Performance Fiber Reinforced Concrete (UHPFRC) is a relative new material with high strength and durability. Some of the main characteristics of UHPFRC are the high compressive strength (normally in the range of 150-200 MPa (21.8-29 ksi)), the high tensile strength which can reach values more than 15 MPa (2.2 ksi), the ductile behavior, and finally the durability and the significantly high energy absorption in the post cracking region.

There are published studies where the behavior of UHPFRC under static loading has been investigated (Kang et al.[1], Kang & Kim[2], Hassan et al.[3], Yoo et al.[4], Nguyen et al.[5]). The effect of the steels fibers amount was examined by Kang et al.[1] (2010) and Yoo et al.[4] (2013) and it was found that the flexural strength was considerably increased as the fiber volume ratio was increased, while the ductility was decreased. Inverse analysis (Kang et al.[1]) was used to determine the direct tensile fracture model of UHPFRC, and a tri-linear tensile fracture model of UHPFRC with a softening branch was proposed. Another important parameter in case of UHPFRC is the orientation and the distribution of steel fibers in the mix.

1   This parameter can considerably affect the post-cracking behavior but the effect on the pre-

2   cracking elastic phase is negligible (Kang & Kim[2]).

3   All these studies are focused on the mechanical properties of UHPFRC under static loading.

4   However, there are not any available studies on the behavior of UHPFRC under cyclic

5   loading, even if the behavior of the material under cyclic loading is of high importance in

6   earthquake prone areas. The main aim of this study is to investigate the behavior of UHPFRC

7   under cyclic loading and to develop a constitutive model for the tensile stress-strain

8   characteristics of the material under cyclic loading. The proposed model is based on

9   previously published models on the cyclic behavior of conventional concrete. Yankelevsky

10   and Reinhardt[6] proposed a stress-strain model for normal concrete under cyclic tension. In

11   this model, using seven geometrical points, the unloading and reloading curves were

12   constructed as linear parts. Yankelevsky and Reinhardt[7] developed a model for concrete

13   subjected to cyclic compression. In this model the same principles as the model of

14   Yankelevsky and Reinhardt[6] for concrete under tension were used. This model was based on

15   the envelope curve which was assumed to be independent of the loading history, and the

16   unloading –reloading curves were composed by linear parts using six focal points. Sima et

17   al.[8] presented a model for the cyclic response of concrete in both tension and compression.

18   The modulus of elasticity and the strength degradation with the cycles were both taken into

19   account, and the reliability of the model under various cyclic loading histories was

20   highlighted. Aslani and Jowkarmeimandi[9] developed a constitutive model for unconfined

21   concrete subjected to cyclic tension and compression. In this model, the unloading curves

22   were considered non-linear, while the reloading curves were considered linear and the

23   degradation of the modulus of elasticity was taken into consideration.

24   Mander et al.[10] proposed a stress-strain relation for reversed loading. For this model, the

25   envelope curve was considered identical to the monotonic stress-strain curve. For the

1   simulation of the monotonic curve a modified equation proposed by Popovic[11] was used. The

2   unloading and reloading branches of the model were calibrated using available experimental

3   results. Martinez-Rueda and Elnashai[12] proposed a modified model based on the model

4   proposed by Mander et al.[10], which takes into consideration strength and modulus of

5   elasticity degradation under increased strain values.

6   In the present study, the results of an extensive experimental program on UHPFRC under

7   direct tensile loading are presented first. Various loading histories and different percentages

8   of steel fibers have been investigated and the stress-axial strain responses have been recorded.

9   These experimental results have been used for the development of a constitutive stress-axial

10   strain model of UHPFRC under cyclic loading. The accuracy of the proposed model is

11   validated using experimental results with various loading histories and for different

12   percentages of steel fibers, while the reliability of the proposed model is highlighted.

13

14   **RESEARCH SIGNIFICANCE**

15   The use of UHPFRC for earthquake resistant structures is a novel application. In earthquake

16   prone areas the structures, and subsequently the load bearing elements, are subjected to

17   seismic loads which are usually simulated with a cyclic loading history. The cyclic response

18   of the structural elements is highly affected by the behavior of the materials under cyclic

19   loading. However, there are not any previously published studies on UHPFRC under cyclic

20   loading. The current study aims to address this research gap by presenting the results of an

21   extensive experimental investigation. These results have been used for the constitutive

22   modeling of the behavior of UHPFRC under cyclic loading. The proposed model can

23   accurately predict the response of UHPFRC under various loading histories and for different

24   percentages of steel fibers while the reliability of the model is evidenced by comparisons with

25   experimental data.

1

2 **EXPERIMENTAL INVESTIGATION**

3 In the current experimental investigation, direct tensile tests of UHPFRC under monotonic

4 and cyclic loading were conducted. Different percentages of steel fibers were examined in

5 order to investigate the effect of the amount of steel fibers on the tensile strength of UHPFRC.

6 Cyclic loading tests under various loading histories were performed and a model for the

7 response of UHPFRC under cyclic loading was proposed. The proposed model was validated

8 for the different loading histories and the different percentages of steel fibers. Detailed

9 description of the material preparation procedure and the experimental setup are presented in

10 the following sections.

11

12 **Mix design and specimens' preparation**

13 One of the main characteristics of UHPFRC is the enhanced homogeneity which is achieved

14 by the use of fine aggregates only. Hence, in the mix silica sand with maximum particle size

15 of 500 μm (0.01969 in) and compacted bulk density of 1587 kg/m^3 (98.4 lb/ft^3) was used

16 together with dry silica fume with bulk density 200-350 kg/m^3 (12.4-21.7 lb/ft^3) and

17 retention on 45 μm (0.00177 in) sieve < 1.5 %, Ground Granulated Blast Furnace Slag

18 (GGBS) with density 2400-3000 kg/m^3 (148.8-186 lb/ft^3) and cement I class 32.5 N. Micro

19 silica with fine particles was used in order not only to increase the density of the matrix but

20 also to improve the rheological properties of the mix. Low water/cement ratio was also used

21 together with polycarboxylate superplasticizer. In the examined mix, 3 different percentages

22 of steel fibers, 1%, 2% and 3% per volume were used. The steel fibers had length 13 mm

23 (0.51181 in), diameter 0.16mm (0.0063 in) , tensile strength 3000 MPa (435 ksi) while the

24 modulus of elasticity had value 200 GPa (29 Msi). The examined mix (Table 1) was based on

25 a previous study (Hassan et al.[3] 2012)

1 Regarding the mixing procedure, all the dry ingredients were mixed initially for 3 minutes.

2 Then, water and superplasticizer were added to the mix and once the mix was wet, steel fibers

3 were added gradually. A high shear mixer (Zyklos Pan Mixer ZZ 75 HE) was used for the

4 mixing of the materials. After the demoulding, the specimens were placed in a water curing

5 tank for 28 days. The specimens were tested 3 months after the casting.

6

7 **Experimental setup**

8 Dog-bone specimens were used for the direct tensile tests. In total, 25 identical dog bone

9 specimens were examined using different percentages of steel fibers and different loading

10 histories. A rectangular cross section at the neck 13mm*50mm (0.512in*1.969in) was used.

11 The geometry of the examined specimens is illustrated in Figure 1. The tests were conducted

12 using Instron 8500 testing machine. The extension was recorded using a Linear Variable

13 Differential Transformer (LVDT) connected to a special steel frame (Figure 2b). This setup

14 was used in order to measure directly the average of the extensions on both sides of the

15 specimens. A number of specimens were also monitored using LaVision Digital Image

16 Correlation System (Figure 2a) and the extension was found to be in perfect agreement with

17 the LVDT measurements. The tests were controlled by the LVDT measurements, using a

18 constant displacement rate of 0.007 mm/sec (0.00028 in/sec). Three different loading

19 histories were used in this investigation (Figure 3). Extension step of 0.2 mm (0.00789 in)

20 was used for loading history 1, while for loading histories 2 and 3 the step was equal to 0.4

21 mm (0.01578 in) and 0.8 mm (0.02367 in) respectively (Figure 3).

22

23 **Experimental results and discussion**

24 Initially, the performance of UHPFRC under monotonic loading was investigated. For this

25 reason, 6 monotonic tests of dog bone specimens with 3% steel fibers were conducted and the

1   stress- axial strain curves together with the average curve are presented in Figure 4. The

2   respective stress-axial strain results for the specimens tested under cyclic loading for the

3   loading histories 1, 2 and 3 are presented in Figures 5a, 5b and 5c respectively. Additionally,

4   in table 2, average stress and axial strain values for characteristic points at the end of the

5   linear part and at the maximum stress are presented. These results (table 2) indicate that there

6   is a significant strain hardening branch from the end of the linear part of the stress-axial strain

7   curve until the ultimate stress value.

8   The experimental results of Figure 5 were used for the calculation of the modulus of elasticity

9   degradation with the number of cycles. The results for all the identical specimens together

10 with the average distributions and the bilinear approximations, for loading histories 1, 2 and 3

11 are presented in Figures 6a, 6b and 6c respectively.

12   From Figure 6 it is evident that the modulus of elasticity was considerably reduced after the

13 first loading cycle in all the examined loading cases and then it was slightly further reduced

14 as the number of cycles was increased. In all the examined cases the modulus of elasticity

15 was approximately reduced to the 25% of its initial value after the first loading cycle. This

16 significant reduction is mainly attributed to the fact that in all the examined loading histories,

17 the response of the specimens reached the post-cracking phase at the first loading cycle

18 (Figure 5).

19 The average curve of all the examined cases is presented in Figure 7. Based on these results

20 (Figure 7), equation 1 is proposed for the reduction of the modulus of elasticity with the

21 loading cycles. This equation was also used for the bilinear approximations of figure 6 and it

22 can be observed that the results obtained using equation 1 are in very good agreement with

23 the experimental results.

24

25 $\frac{E_n}{E_0} = (0.25 - 0.016 \cdot n)$ (1)

1

2   where:

3   n: is the number of cycles, n>1

4   E_0: is the initial modulus of elasticity,

5   E_n: is the modulus of elasticity after n cycles.

6

7   The comparison between the average experimental results and the proposed model is

8   presented in Figure 8. The results of the bilinear models indicate that the behavior is not

9   affected by the loading history and is governed by the same equation 1 in all the examined

10   cases.

11

12   **ANALYTICAL INVESTIGATION**

13   The response of UHPFRC in direct tension is dissimilar to the response of conventional plain

14   concrete under the same loading condition. The behavior of concrete in tension is considered

15   linear up to the maximum level of stress and after this point a sudden failure occurs. On the

16   contrary, for UHPFRC after the linear part in which the steel fibers don't have any effect, the

17   first crack appears and we have a non-linear behavior up to the maximum load. After this

18   point the stress drops gradually. These phases of UHPFRC under tension can be distinguished

19   in figure 9.

20   In the present study, the envelope curve for cyclic loading is assumed identical to the

21   monotonic stress-axial strain response. This assumption has also been adopted by other

22   researchers (Yankelevsky and Reinhardt[6] and Bahn and C. T. Hsu[13]). In figure 10 the

23   average monotonic curve is presented together with the respective results of cyclic loading

24   tests. The results indicate that the average monotonic curve is approaching the cyclic

25   response of the specimens.

1 The proposed model is consisted of 5 various phases as presented in figure 9. The first is the

2 linear phase up to a level of stress f_0 and axial strain ε_0. The second is the non-linear phase up

3 to a maximum stress of f_c and axial strain ε_c. The third is the descending phase until the

4 unloading point (f_{un}, ε_{un}), and finally the next 2 phases are the unloading and the reloading

5 phases. In the first part, the stress-strain relation is linear, hence it is given from the equation

6 2.

7

$$\sigma = \varepsilon \cdot E_0 \quad \text{for } \varepsilon \leq \varepsilon_0 \tag{2}$$

8

9 where:

10 ε: is the axial strain,

11 E_0 : is the modulus of elasticity,

12

13 After the elastic part, the behavior of the material is characterized by an ascending non-linear

14 branch until the maximum stress. This is the phase where the cracking of the concrete matrix

15 occurs and the steel fibers are bridging the micro-cracks. After this point, the stress falls

16 gradually due to the localization of the damage. This non-linear behavior is described by an

17 exponential curve. Hence, two equations are proposed for both the ascending part (from the

18 elastic limit until the maximum stress limit), as well as the descending branch from the

19 maximum stress limit up to the unloading point. Therefore, for the ascending part the

20 following equation 3 is proposed:

21

$$\sigma = \varepsilon_0 \cdot (1-A) + A \cdot \varepsilon \cdot e^{\frac{(\varepsilon_0 - \varepsilon)}{\varepsilon_c}} \tag{3}$$

22

23 where:

1   ε_0: is the axial strain at the end of the linear part,

2   ε_c: is the respective axial strain for the maximum stress,

3

4   A is given from the equation (4).

$$A=\frac{f_c - \varepsilon_0 \cdot E_0}{E_0 \cdot (\varepsilon_c \cdot e^{(\frac{\varepsilon_0}{\varepsilon_c}-1)} - \varepsilon_0)} \qquad (4)$$

5   where f_c is the maximum stress

6

7   These equations were initially proposed by Mazars and G. Pijaudier-Cabot[14] and they were

8   also used by other researchers (Sima et al.[8], Faria et al.[15], Saetta et al.[16]).

9   For the descending branch and taking into consideration the softening part, Sima et al.[8]

10   considered an exponential curve and took into consideration a point on the envelope curve.

11   This exponential curve is also adopted for UHPFRC in the descending branch. Therefore, the

12   descending curve is described by the equation 5:

13

$$\sigma=(B+C\cdot\varepsilon\cdot e^{(\frac{\varepsilon_0-\varepsilon}{\varepsilon_c})})\cdot E_0 \ \text{ for } \varepsilon>\varepsilon c \qquad (5)$$

14

15   where:

$$B=\frac{f_{op}\cdot\varepsilon_c\cdot e^{(\frac{\varepsilon_0}{\varepsilon_c}-1)} - \varepsilon_{op}\cdot f_c\cdot e^{\frac{\varepsilon_0}{\varepsilon_c}\cdot(1-\frac{\varepsilon_{op}}{\varepsilon_0})}}{E_0\cdot(\varepsilon_c\cdot e^{(\frac{\varepsilon_0}{\varepsilon_c}-1)} - \varepsilon_{op}\cdot e^{\frac{\varepsilon_0}{\varepsilon_c}\cdot(1-\frac{\varepsilon_{op}}{\varepsilon_0})})} \qquad (6)$$

$$C=\frac{f_c - f_{op}}{E_0\cdot(\varepsilon_c\cdot e^{(\frac{\varepsilon_0}{\varepsilon_c}-1)} - \varepsilon_{op}\cdot e^{\frac{\varepsilon_0}{\varepsilon_c}\cdot(1-\frac{\varepsilon_{op}}{\varepsilon_0})})} \qquad (7)$$

16

1   where:

2   ε_{op}: is the axial strain at any point on the descending part of the stress-axial strain curve,

3   f_{op}: is the respective stress at any point on the descending part of the stress-axial strain curve.

4

5   Previous studies on plain concrete (Sinha et al.[17]) indicate that during the unloading phase,

6   the modulus of elasticity is high at the beginning, then gradually drops, and finally becomes

7   flat. Based on the experimental results of the present study, the unloading branch of UHPFRC

8   exhibits a different behavior which is attributed to the presence of steel fibers in the mix. For

9   this reason, the experimental results have been used for the calibration of the constitutive

10   model. The equation proposed by Sima et al.[8] for the unloading part has been calibrated in

11   order to fit the experimental results (equation 8). From the validation of the proposed model

12   and using all the experimental results of the various mixes it was evident that this equation

13   can accurately predict the behavior of UHPFRC in this branch.

14

$$\sigma = D \cdot e^{\dfrac{F \cdot \left(1 - \frac{\varepsilon - \varepsilon_{pl}}{\varepsilon_{un} - \varepsilon_{pl}}\right)}{22}} \cdot E_0 \cdot (\varepsilon - \varepsilon_{pl}) \tag{8}$$

15

16   where :

$$D = \frac{r \cdot (1 - \delta_{un})}{r - 1} \tag{9}$$

$$r = \frac{\varepsilon_{un}}{\varepsilon_{pl}} \tag{10}$$

17

18   ε_{pl}: is the residual axial strain for the unloading curve for zero stress,

19   ε_{un}: is the unloading axial strain,

1   δun: is the compressive damage at the unloading point and is given from equation (11).

2

$$\delta_{un} = 1 - \frac{B}{\varepsilon} - C \cdot e^{(\frac{\varepsilon_0 - \varepsilon}{\varepsilon_c})}$$ (11)

3   F is given from the equation (12).

4

$$F = Ln(\frac{R \cdot (1-\delta_{un}) \cdot (r-1)}{r})$$ (12)

5

6   R is given from the equation (13)

7

$$R = \frac{E_{pl}}{E_0}$$ (13)

8   where E_{pl} is the Modulus of elasticity at the end of the unloading curve.

9

10   The experimental results presented in this study indicate that the modeling of the re-loading

11   part with a linear stress-strain equation, which is adopted for conventional concrete, can't

12   accurately predict the response of UHPFRC. Hence, an exponential equation, which is a

13   modification of equation 3, is proposed in order to describe the behavior of the reloading

14   curves of UHPFRC (Equation 14).

$$\sigma = (\varepsilon_{0'} \cdot (1-A') + A' \cdot \varepsilon \cdot e^{(\frac{\varepsilon_{0'} - \varepsilon}{\varepsilon_{c'}})}) \cdot E_{0'}$$ (14)

15

16   where:

17   A: is given from the equation (15)

$$A' = \frac{f_{c'} - \varepsilon_{0'} \cdot E_{0'}}{E_{0'} \cdot \left(\varepsilon_{c'} \cdot e^{\left(\frac{\varepsilon_{0'}}{\varepsilon_{c'}} - 1 \right)} - \varepsilon_{0'} \right)} \tag{15}$$

1

2    $f_{c'}$: is the maximum stress at the reloading curve,

3    $\varepsilon_{c'}$: is the axial strain for the respective maximum stress in the descending curve,

4    $\varepsilon_{c'} = \varepsilon - \varepsilon_{pl,}$

5    $E_{0'}$: is the initial tangent modulus of elasticity,

6    $\varepsilon_{0'}$: is the respective maximum strain for the tangent modulus of elasticity.

7

8   **VALIDATION OF THE PROPOSED CONSTITUTIVE MODEL**

9   Experimental results of all the examined loading histories for specimens with 3% steel fibers

10   were used for the validation of the model. In figures 11a, 11b and 11c the results of the

11   proposed constitutive model are compared with experimental results for loading histories 1, 2

12   and 3 respectively. From these figures it is evident that the results of the proposed model are

13   in very good agreement with the respective experimental results. Therefore, it can be

14   concluded that the proposed model can accurately predict the cyclic response of UHPFRC.

15   The required parameters of the proposed model (i.e. the modulus of elasticity and the stress

16   and axial strain at the end of the elastic part and at the maximum stress level) can be

17   calculated from the monotonic stress-axial strain results. For the degradation of the modulus

18   of elasticity with the loading cycles, the proposed model of equation 1 can be adopted, which

19   was validated in the previous section (figure 8).

20

21   **INVESTIGATION OF THE EFFECT OF DIFFERENT PERCENTAGES OF STEEL**

22   **FIBERS**

23   **Effect of steel fibers on the tensile strength of UHPFRC**

1 An additional investigation was conducted on the effect of steel fibers volume on the

2 behavior of UHPFRC. Specimens with percentages 1% and 2% were tested under monotonic

3 loading additionally to the specimens with 3% steel fibers (Table 1). Higher percentages of

4 steel fibers were not investigated since the use of higher steel fiber volumes is not a cost

5 effective way to achieve superior mechanical properties. This was also highlighted by Ferrara

6 et al.[18]. According to this study (Ferrara et al.[18]), high mechanical properties can be achieved

7 even with low percentage of fibers (around 1%) by controlling steel fiber orientation.

8 The experimental results for all the examined mixes together with the average monotonic

9 curves are presented in figures 12 and 13. Also, the average values for the stress and axial

10 strain at the end of the elastic part and at the maximum stress level for the specimens with

11 steel fibers volume 1% and 2% are presented in tables 3 and 4 respectively.

12 From tables 2, 3 and 4, it is evident that the elastic part is not affected by the volume of steel

13 fibers in the mix. Also, it is obvious that as the steel fiber percentage is increased, the

14 maximum stress value is improved and the strain hardening phase is increased. The same

15 observation can be made from the results presented in figure 14. In this figure, the increment

16 of the tensile strength with the steel fibers volume is presented. The experimental results

17 indicate that when steel fibers volume was increased from 1% to 2%, tensile strength

18 increment of 23.1% was observed. Further increment of steel fibers volume from 2% to 3%

19 resulted in 4.3% increment of the maximum tensile strength.

20

21 **UHPFRC under cyclic loading for different percentages of steel fibers**

22 The results of the previous section indicated that strain hardening behavior can be achieved

23 with a minimum percentage of steel fibers 2%. Hence, in order to investigate the reliability of

24 the proposed model for percentages other than 3%, cyclic loading tests (loading history 2,

25 figure 3) were conducted for specimens with 2% steel fibers.

1   The experimental results are presented in figure 15 and the validation of the proposed model

2   is presented in figure 16. From figure 16 it is evident that the proposed model can accurately

3   predict the response of UHPFRC for percentage of steel fibers 2%.

4   **CONCLUSIONS**

5   In the present study, the response of various UHPFRC mixes under tensile monotonic and

6   cyclic loading was investigated.

7   Monotonic tests were conducted on specimens with 1%, 2% and 3% steel fibers volume, and

8   the experimental results indicated that when steel fibers volume was increased from 1% to

9   2%, tensile strength increment of 23.1% was observed. Further increment of steel fibers

10 volume from 2% to 3% resulted to 4.3% increment of the maximum tensile strength. From

11 this investigation it was evident that the elastic part was not affected by the volume of steel

12 fibers, while the strain hardening phase was increased. Based on these results, strain

13 hardening behavior was achieved using 2% minimum percentage of steel fibers. This was the

14 minimum percentage which was used in the current study for specimens tested under cyclic

15 loading.

16 Specimens with 2% and 3% of steel fibers were tested under cyclic loading and a constitutive

17 model for the tensile stress versus axial strain under cyclic loading was proposed. The

18 accuracy of the model was validated using experimental results of specimens with various

19 percentages of steel fibers tested under different loading histories, and the reliability of the

20 proposed model was highlighted. The experimental results of the present study were also

21 used for the calculation of the modulus of elasticity degradation with the number of loading

22 cycles. The results indicated that the modulus of elasticity was considerably reduced after the

23 first loading cycle in all the examined loading cases, and then it was slightly further reduced

24 as the number of loading cycles was increased. Based on these results, a model for the

25 reduction of the modulus of elasticity with the loading cycles was proposed.

1

8

9 **NOTATION:**

10 ε :The axial strain in the linear part.

11 E_0 : The modulus of elasticity.

12 ε_0 :The axial strain at the end of the linear part.

13 ε_c :The respective axial strain for the maximum stress.

14 fc :The maximum stress.

15 ε_{op} : The axial strain at any point on the descending part of the stress-strain curve.

16 f_{op} : The stress at any point on the descending part of the stress-strain curve.

17 ε_{pl} :The residual axial strain for the unloading curve for no stress.

18 ε_{un} :The unloading axial strain.

19 δ_{un} : The damage at the unloading point.

20 E_{pl} :The modulus of elasticity at the end of the unloading curve.

21 $f_{c'}$:The maximum stress at the reloading curve.

22 $\varepsilon_{c'}$:The axial strain for the respective maximum stress in the descending curve and $\varepsilon_{c'}=\varepsilon-\varepsilon_{pl}$

23 $E_{0'}$:The initial tangent modulus of elasticity at the beginning of the reloading curve.

24 $\varepsilon_{0'}$:The respective maximum axial strain for the tangent modulus of elasticity.

25

REFERENCES

1. Kang, S.T., Lee, Y., Park Y.D. and Kim, J.K., "Tensile fracture properties of an Ultra High Performance Fiber Reinforced Concrete (UHPFRC) with steel fiber." Composite Structures, V.92 , No 1, 2010, pp 61-71.

2. Kang, S.T. and Kim, J.K. "The relation between fiber orientation and tensile behavior in an Ultra High Performance Fiber Reinforced Cementitious Composites (UHPFRCC)." Cement and Concrete Research, V. 41, No.10, 2011, pp. 1001-1014.

3. Hassan, A.M.T., Jones, S.W. and Mahmud, G.H. "Experimental test methods to determine the uniaxial tensile and compressive behavior of Ultra High Performance Fiber Reinforced Concrete (UHPFRC)." Construction and Building Materials, V.37, 2012, pp.874-882.

4. Yoo, D.Y., Park, J.J, Kim, S.W. and Yoon, Y.S., "Early age setting, shrinkage and tensile characteristics of ultra high performance fiber reinforced concrete." Construction and Building Materials, V.41, 2013, pp. 427-438.

5. Nguyen, D.L., Kim, J.K, Ryu, G.S. and Koh, K.T., "Size effect on flexural behavior of ultra-high-performance hybrid fiber-reinforced concrete." Composites Part B: Engineering, V.45, No.1, 2013, pp.1104-1116.

6. Yankelevsky, D. Z. and Reinhardt, H.W., "Uniaxial Behavior of Concrete in Cyclic Tension." Journal of Structural Engineering, V.115, No1.,1989.

7. Yankelevsky, D.Z. and Reinhardt, H.W., "Model for Cyclic Compressive Behavior of Concrete." Journal of Structural Engineering V. 113, No.2, 1987.

8. Sima, J.F., Roca, P. and Molins, C,. "Cyclic Constitutive Model for Concrete." Engineering Structures, V.30, No.3, 2008, pp. 695-706.

9. Aslani, F. and Jowkarmeimandi, R., "Stress-strain model for concrete under cyclic loading." Magazine of Concrete Research, V.64, No.8, 2012, pp. 673-685.

10. Mander, J.B., Priestley, M.J and Park, R. "Theoretical Stress-Strain Model for Confined Concrete." Journal of Structural Engineering, V.114, No.8.,1988.

11. Popovics, S., (1973)"A numerical approach to the complete stress-strain curves for concrete",Cement and Concr. Res.,Vol.3, No.5, 1973, pp.583-599.

12. Martinez-Rueda, J.E. and Elnashai, A.S., "Confined Concrete model under cyclic load " Material and Structures, V.30, 1997, pp. 139-147.

13. Bahn, B. Y. and Hsu, C.T "Stress-strain behavior of concrete under cyclic loading." ACI Materials Journal, V.95, No.2, 1998,pp.178-193.

14. Mazars, J. and Pijaudier-Cabot, G. (1989). "Continuum damage theory. Application to concrete." Journal of Engineering Mechanics, V.115, No.2, 1998, pp. 345-365.

15. Faria, R., Oliver, J. and Cervera, M., "A strain based plastic viscous -damage model for massive concrete structures." International Journal of Solids and Structures , V.34 No.14, 1999, pp. 1533-1558.

16. Saetta, A., Scotta, R. and Vitaliani, R., "Coupled Environmental -Mechanical damage model of RC structures." Journal of Engineering Mechanics , V.128, No.8, 1999, pp. 930-940.

17. Sinha, B.P., Gerstle, K.H. and Tulin, L.G. "Stress-Strain Relations for Concrete Under Cyclic Loading." Journal of American Concrete Institute V.61, No.2., 1964.

1 18. Ferrara, L. , Ozyurt, N., Di Prisco, M., "High mechanical performance of fibre

2 reinforced cementitious composites: the role of "casting-flow induced" fibre orientation."

3 Material and Structures 2011, V.44, No1, pp. 109-128.

4

5 **TABLES AND FIGURES**

6 **List of Tables:**

11

12 **List of Figures:**

1   **Figure 11-** Validation of the proposed model using experimental results for 3 different

2   loading histories and 3% steel fibers

3   **Figure 12-** Monotonic stress-axial strain curves for specimens with 1% steel fibers

4   **Figure 13-** Monotonic stress-axial strain curves for specimens with 2% steel fibers

5   **Figure 14-** Tensile strength for different percentages of steel fibers

6   **Figure 15-** Stress-axial strain curves of UHPFRC with 2% steel fibers under cyclic loading

7   **Figure 16-** Validation of the proposed model for percentage of steel fibers 2%

8

9   **Table 1 – UHPFRC mix design for specimens with different percentages of steel fibers**

Material	Mix proportions (kg/m^3)		
Cement	657		
GGBS	418		
Silica fume	119		
Silica Sand	1051		
Superplasticizers	59		
Water	185		
Steel fibers (13mm length (0.5118 in) and 0.16 mm (0.0063 in) diameter)	235.5 (3% Steel fibers)	157 (2% steel Fibers)	78.5 (1% steel fibers)

16   Note: 1 kg/m^3=0.062 lb/ft^3 and 1mm=0.03937 in

17

18   **Table 2 –Average stress and axial strain values for specimens with 3% steel fibers**

Stress Level	Stress (MPa)	Axial Strain
End of Elastic	6.3	0.00013
Maximum Stress	8.9	0.01

22   Note: 1MPa= 0.145 ksi

1

Table 3–Average stress and axial strain values for specimens with 1% steel fibers

Stress Level	Stress (MPa)	Axial Strain
End of Elastic	6.0	0.00014
Maximum Stress	6.6	0.0008

Note: 1MPa= 0.145 ksi

Table 4–Average stress and axial strain values for specimens with 2% steel fibers

Stress Level	Stress (MPa)	Axial Strain
End of Elastic	7.0	0.00015
Maximum Stress	8.1	0.00094

Note: 1MPa= 0.145 ksi

1
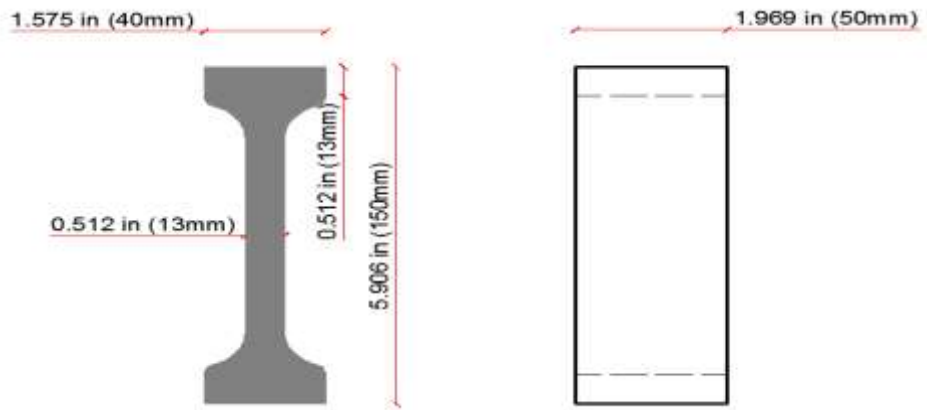
(Note: 1 mm=0.03937 in)

Figure 1 - Dog bone specimen

5

6

(a)   **(b)**
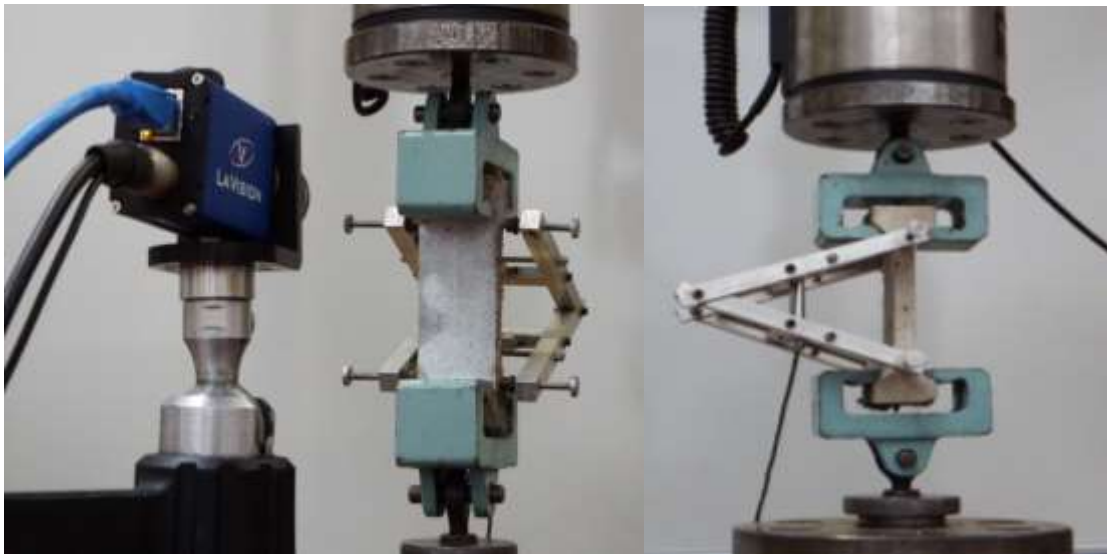
Figure 2-Experimental setup

10

11

12

1

2
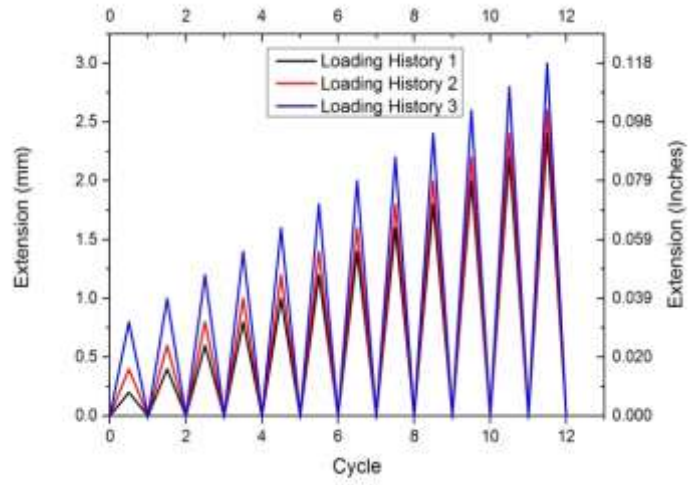
(Note: 1 mm=0.03937 in)

Figure 3- Examined loading histories

5

6

7
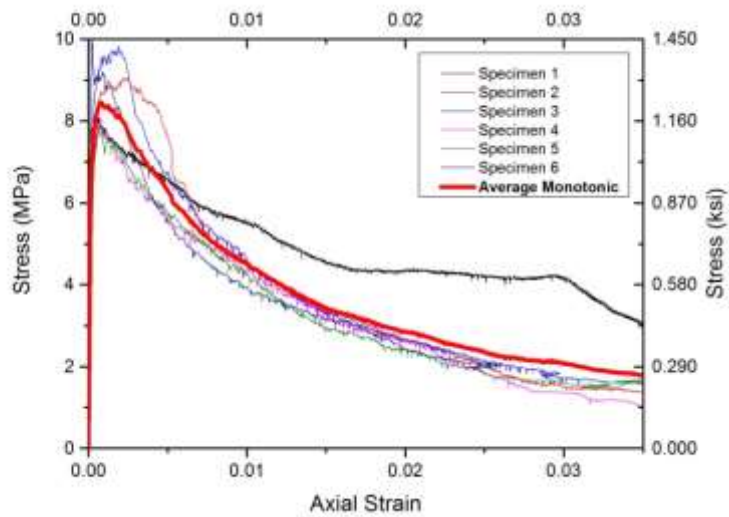
(Note: 1MPa= 0.145 ksi)

Figure 4- Monotonic stress-axial strain curves for specimens with 3% steel fibers

11

1

2   (a)

3

4   (b)

5

6   (c)
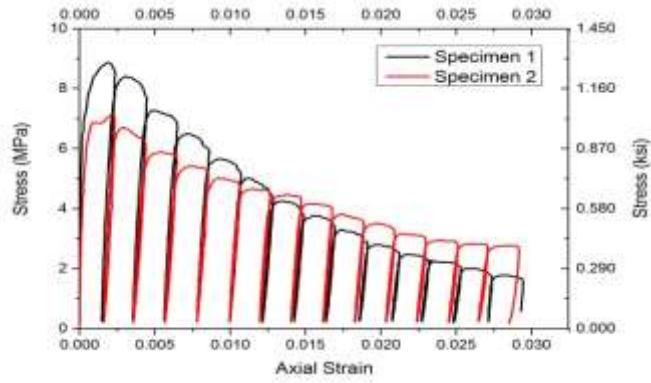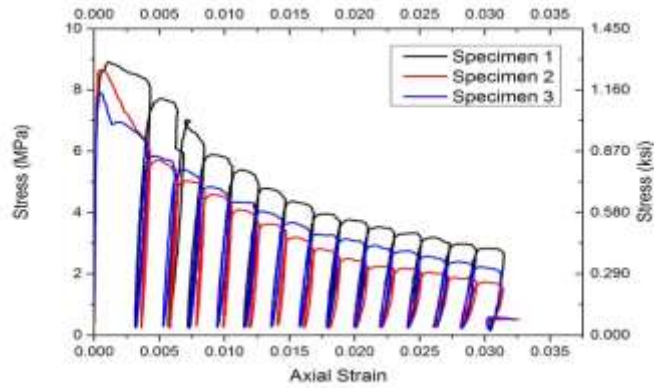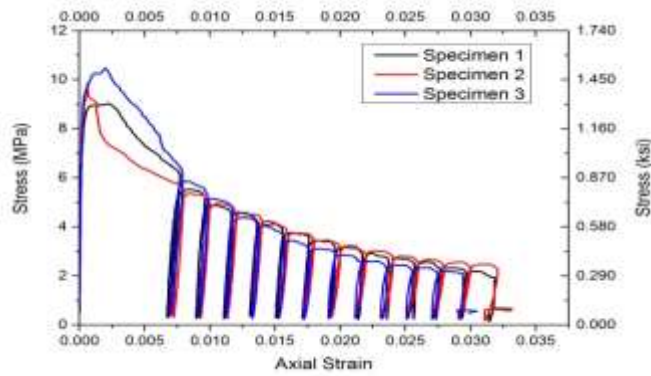
7   (Note: 1MPa= 0.145 ksi)

8   **Figure 5– Experimental results for a) loading history 1, b) loading history 2,**

9   **and c) loading history 3**

1

2   (a)

3

4   (b)

5

6   (c)
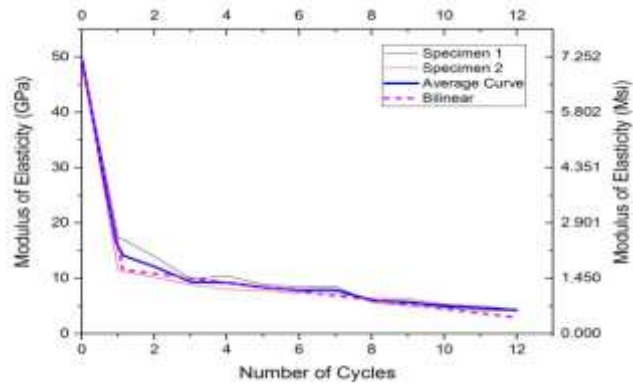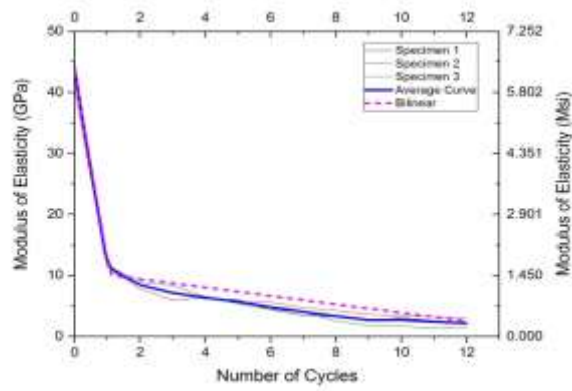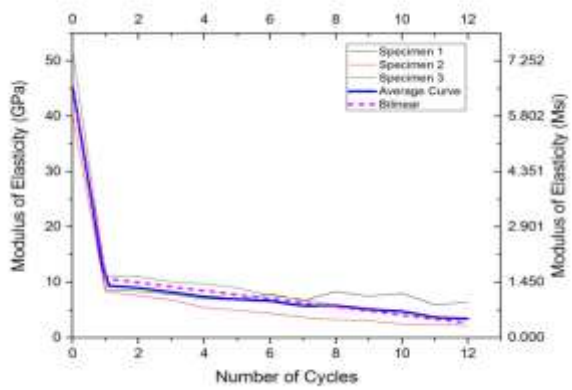
7   (Note: 1 GPa=0.145 Msi)

8   **Figure 6– Modulus of elasticity degradation for a) loading history 1 b) loading**

9   **history 2 c) loading history 3**

1

2
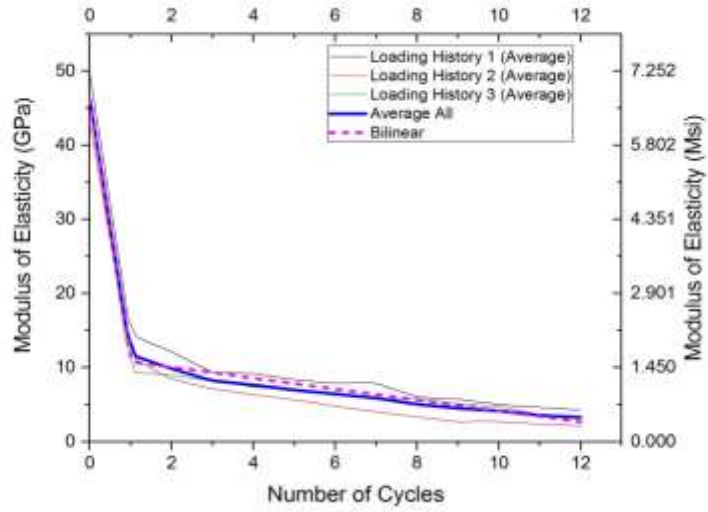
(Note: 1 GPa=0.145 Msi)

Figure 7- Average curves of the modulus of elasticity degradation for all the loading histories

6

7
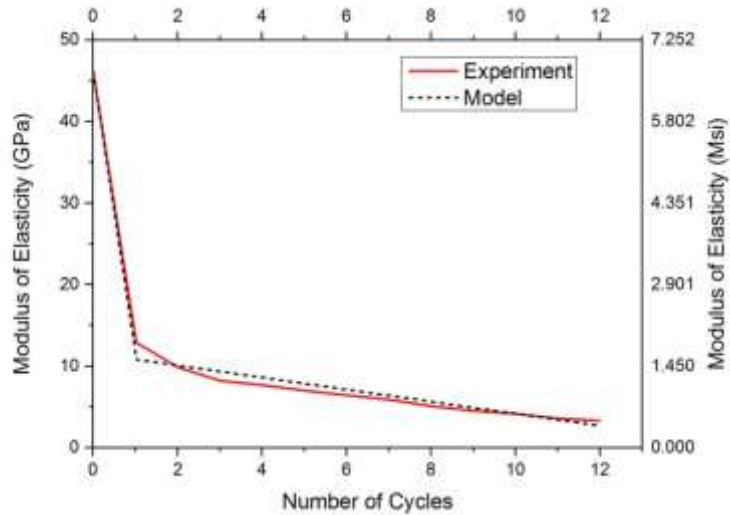
(Note: 1 GPa=0.145 Msi)

Figure 8- Degradation of the modulus of elasticity with the loading cycles

10

1
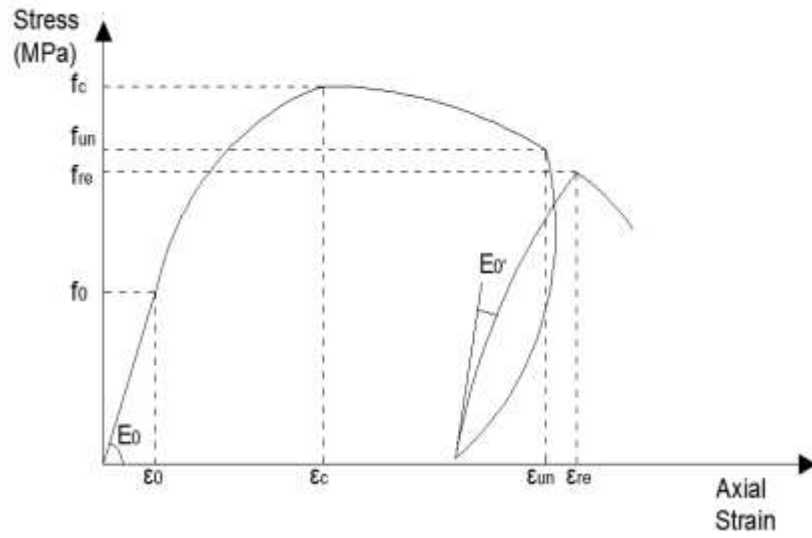
2   **Figure 9- Stress-Axial Strain Curve of UHPFRC under cyclic loading**

3   (Note: 1MPa= 0.145 ksi)

4

5

6
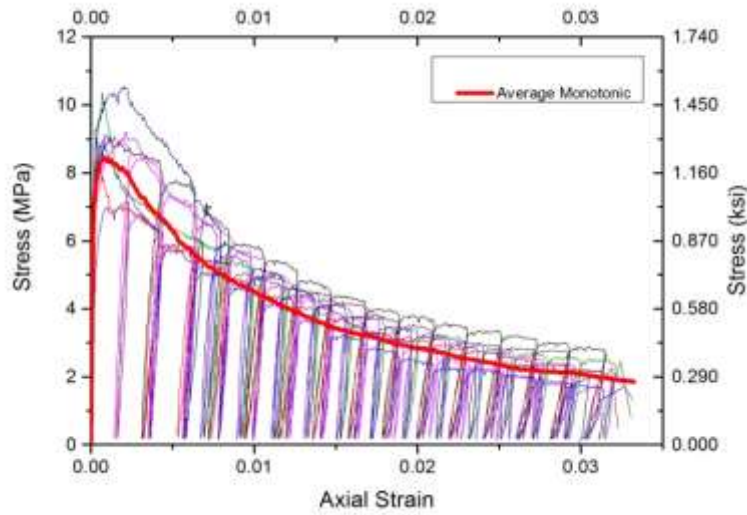
7   (Note: 1MPa= 0.145 ksi)

8   **Figure 10- Comparison of the average monotonic curve with the cyclic envelope curves**

9

10

1

2
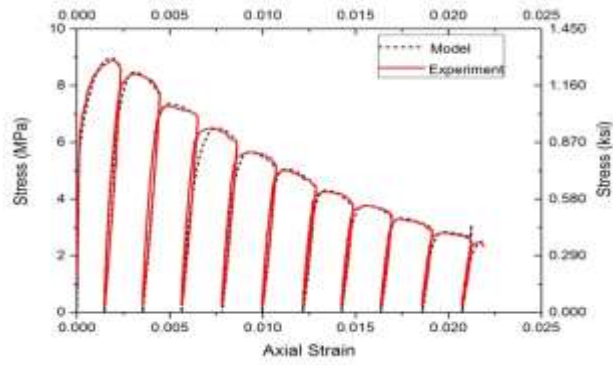
3

4   (a)
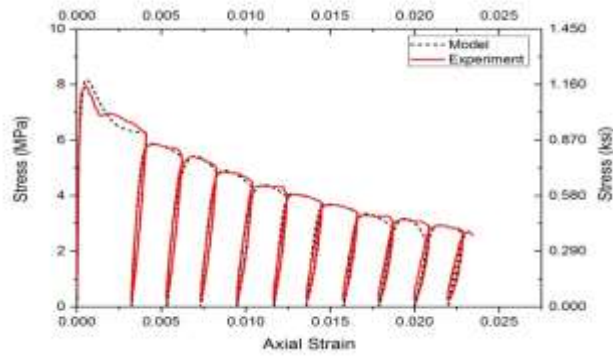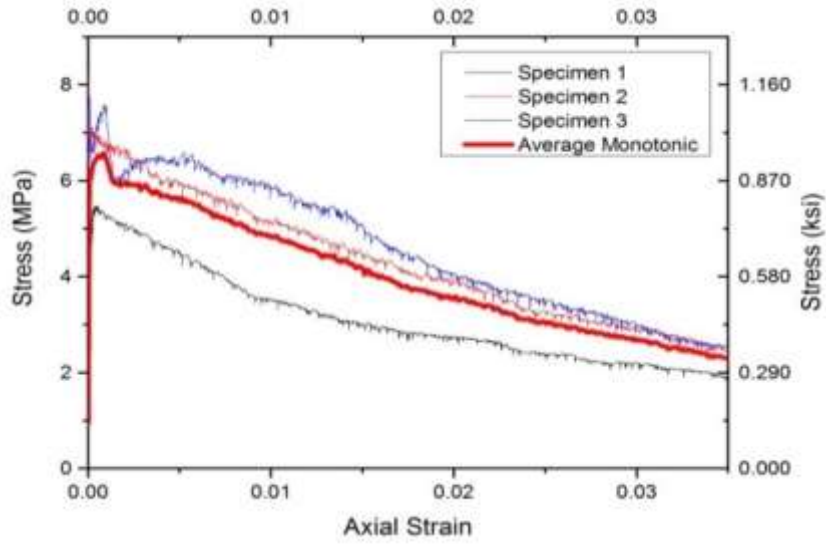

5

6   (b)
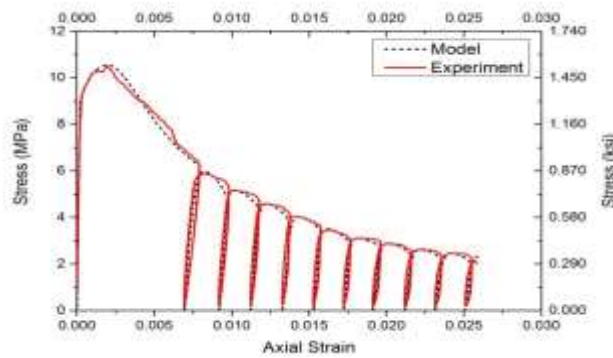
7

8   (c)

9   (Note: 1MPa= 0.145 ksi)

10   **Figure 11- Validation of the proposed model using experimental results for 3 different**

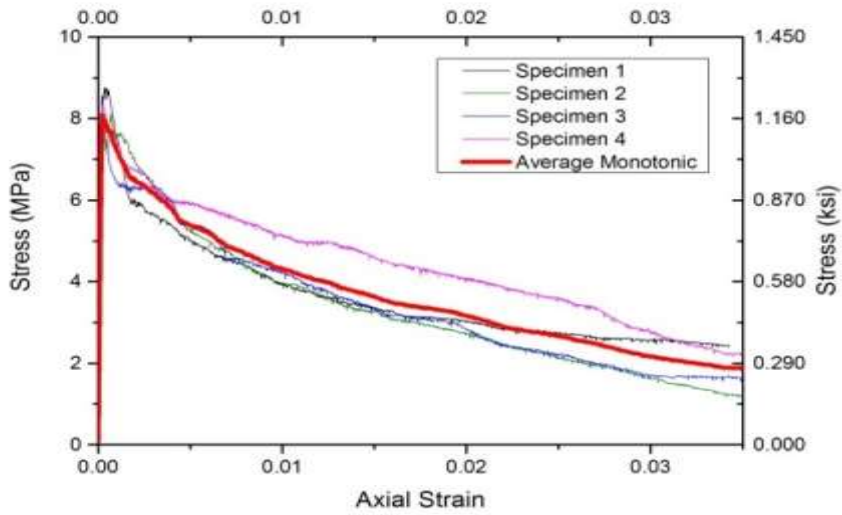11   **loading histories and 3% steel fibers**

1

2

(Note: 1MPa= 0.145 ksi)

Figure 12- Monotonic stress-axial strain curves for specimens with 1% steel fibers
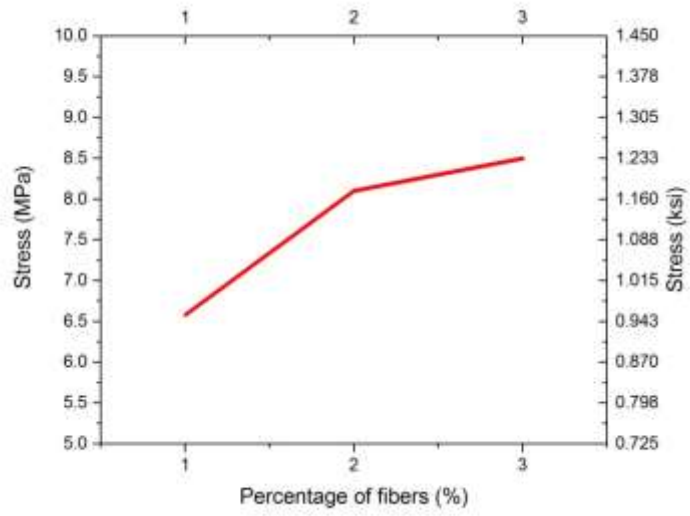
5

6

7

(Note: 1MPa= 0.145 ksi)

Figure 13- Monotonic stress-axial strain curves for specimens with 2% steel fibers
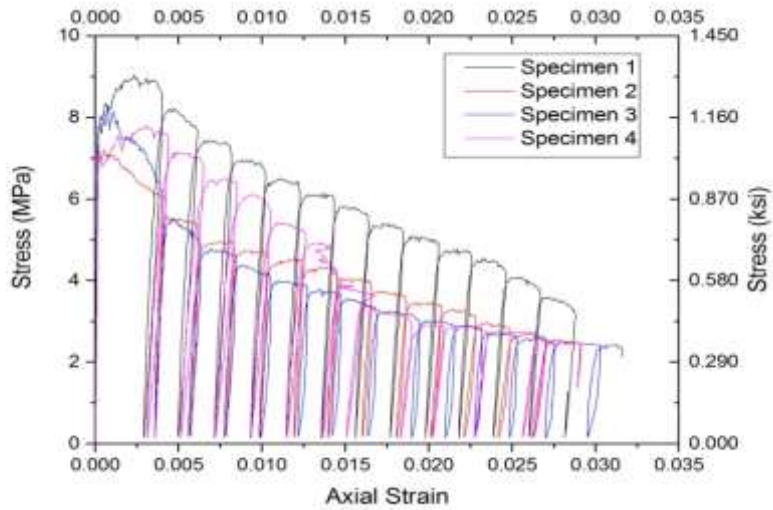
10

1

2

3

(Note: 1MPa= 0.145 ksi)

Figure 14- Tensile strength for different percentages of steel fibers

6

7

8
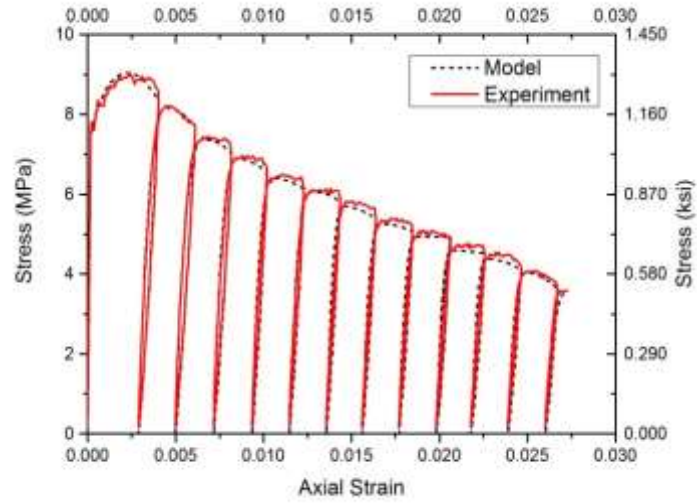
(Note: 1MPa= 0.145 ksi)

1   **Figure 15- Stress-axial strain curves of UHPFRC with 2% steel fibers under cyclic**

2   **loading**

3

4

5   (Note: 1MPa= 0.145 ksi)

6   **Figure 16-Validation of the proposed model for percentage of steel fibers 2%**

7